Bioorganic & Medicinal Chemistry 19 (2011) 7049–7056

Contents lists available at SciVerse ScienceDirect

Bioorganic & Medicinal Chemistry

journal homepage: www.elsevier.com/locate/bmc

Screening of a library of T7 phage-displayed peptides identifies alphaC helix in 14-3-3 protein as a CBP501-binding site

Yuki Matsumoto [a], Yosuke Shindo [a], Yoichi Takakusagi [a,†], Kaori Takakusagi [a], Senko Tsukuda [a], Tomoe Kusayanagi [a], Hitoshi Sato [b], Takumi Kawabe [b], Fumio Sugawara [a], Kengo Sakaguchi [a,*]

[a] Department of Applied Biological Sciences, Faculty of Science and Technology, Tokyo University of Science, 2641 Yamazaki, Noda, Chiba 278-8510, Japan
[b] CanBas. Co. Ltd, 2-2-1 Otemachi, Numazu, Shizuoka 410-0801, Japan

ARTICLE INFO

Article history:
Received 28 September 2011
Accepted 4 October 2011
Available online 7 October 2011

Keywords:
CBP501
G2 checkpoint
T7 phage display
Peptide
14-3-3ε

ABSTRACT

CBP501 is a chemically modified peptide composed of twelve unnatural D-amino acids, which inhibits Chk kinase and abrogates G2 arrest induced by DNA-damaging agents. Here we identified an alphaC helix in 14-3-3 protein as a CBP501-binding site using T7 phage display technology. An affinity selection of T7 phage-displayed peptide using biotinylated CBP501 identified a 14-mer peptide NSDCIISRKIEQKE. This peptide sequence showed similarity to a portion of the alphaC helix of human 14-3-3ε, suggesting that CBP501 may bind to this region. Surface plasmon resonance (SPR) and ELISA demonstrated that CBP501 interacts with 14-3-3ε specifically at the screen-guided region. An avidin-agarose bead pull-down assay showed that CBP501 also binds to other 14-3-3 isoforms in Jurkat cells. Among the other known Chk kinase inhibitors tested, CBP501 showed the strongest affinity for 14-3-3ε. Thus, we conclude that in addition to the direct inhibition of Chk kinase activity, CBP501 directly binds to cellular 14-3-3 proteins through alphaC helix.

1. Introduction

In eukaryotes, the cell cycle can be divided into two main phases: (i) interphase, during which the cell grows, duplicates its DNA and prepares for mitosis and (ii) the mitotic (M) phase, during which the cell divides into two distinct cells. Interphase proceeds in three stages, G1, S and G2 phase. Cell-cycle progression is regulated by several checkpoints if previous events have not been completed.[1,2] In eukaryotic cells, two main checkpoints exist, namely G1 and G2.[3,4] These checkpoints respond to possible damage by arresting the cell cycle to provide time for repair and by inducing transcription of appropriate genes. The G1 and G2 checkpoint pathways allow cells to deal with both endogenous and exogenous sources of DNA damage.

The relationship between carcinogenesis and cell-cycle control is well documented.[3–5] Normal cells repair the damaged DNA at both the G1 or G2 checkpoints, whereas most cancer cells have mutations in several tumor suppressor genes involved in the G1 checkpoint such as p53 and Rb.[6–10] Therefore, such cancer cells perform DNA repair only during the G2 checkpoint instead of the G1 checkpoint. If the G2 checkpoint in these cancer cells is forcibly abrogated, the loss of both checkpoints lead to a failure of cells to repair the DNA damage, resulting in the loss of cell viability.

It is well known that G2 arrest is primarily induced by two independent cascades that are activated in response to DNA damage and following activation of ATM/ATR.[3,11] One is the inhibitory phosphorylation of the Cdc25 family by Chk1 and Chk2 that are in turn phosphorylated by ATM/ATR. The phosphorylated Cdc25 is recognized by 14-3-3 protein and removed from nucleus to cytosol. Thus, phosphorylated Cdc25 can no longer activate the cdc2–cyclinB complex in the nucleus and stop the cell cycle at the G2 phase.[11–13] The other cascade is the phosphorylation of p53 by ATM/ATR, which stimulates transcription of 14-3-3σ and inhibits the function of the cdc2–cyclinB complex by nuclear exclusion of cdc2.[14–16]

In both cascades described above, 14-3-3 proteins play a role in the G2 checkpoint.[17,18] The 14-3-3 family of proteins are highly conserved and ubiquitously expressed in all eukaryotic species.[15,19] In mammals, there are seven isoforms of 14-3-3: β, γ, ε, η, σ, τ and ζ. 14-3-3 proteins form homo- or hetero-dimers by interacting with a large number of proteins in an isoform specific manner.[17,18,20] For example, it has been reported that γ and ε subtypes are important in the Cdc25C-mediated pathway by directly binding to S216-phosphorylated Cdc25C and thereby promoting migration from the nucleus to the cytosol for the G2/M transition.[19,21–24] In contrast, only the σ isoform plays a central role in the p53-mediated cascade.[14–16] Association of Chk1 or Wee1 with 14-3-3 proteins is also a key event at the G2 checkpoint, although the precise mechanism

* Corresponding author. Tel.: +81 4 7124 1501x5009; fax: +81 4 7123 9767.
E-mail address: kengo@rs.noda.sut.ac.jp (K. Sakaguchi).
† Present address: National Cancer Institute, National Institutes of Health, Bethesda, MD, USA.

0968-0896/$ - see front matter © 2011 Elsevier Ltd. All rights reserved.
doi:10.1016/j.bmc.2011.10.004

or functional role of each 14-3-3 isoform needs to be clarified.[25–30] In previous studies on the G2 checkpoint, several compounds that target mediators of the G2 checkpoint have been reported; Chk1 (UCN-01, debromohymenialdisine (DBH), SB218078, TAT-S216A), Chk2 (DBH, TAT-S216A), ATM/ATR (caffeine) and Wee1 (PD01 66285). These compounds are known to abrogate G2 arrest induced by DNA damage. However, G2 abrogators that target 14-3-3 proteins have never been reported.[31]

CBP501 is a chemically modified peptide composed of twelve unnatural D-amino acids, which was optimized as a G2 checkpoint inhibitor based on TAT-S216A by CanBas Co. Ltd (Shizuoka, Japan) and is currently in clinical practice.[32–34] This peptide inhibits the Chk1/Chk2 kinase in vitro and abrogates G2 arrest induced by DNA-damaging agents at the cellular level in much lower concentration than that for the inhibitory concentration of Chk kinase.[32] These data suggest that there may be molecular targets other than Chk1/Chk2.[32]

T7 phage display technology is a powerful molecular biological tool that allows determination of the targets for small-molecule therapeutics.[35] Here, we describe the screening of a library of T7 phage-displayed peptides to identify CBP501-binding targets. Our results show CBP501 binds the alphaC helix in 14-3-3ε. The interaction between CBP501 and 14-3-3 was subsequently validated using surface plasmon resonance (SPR) analysis, ELISA and pull-down assay. Furthermore, a pull-down assay using Jurkat cells, which lack the p53-mediated pathway at the G2 checkpoint, was carried out to demonstrate that CBP501 binds to all 14-3-3 isoforms present in these cells. Moreover, binding of the well-known Chk kinase inhibitors to 14-3-3ε were also tested and their respective affinity compared with that of CBP501.

2. Materials and methods

2.1. Chemicals and antibodies

CBP501 and a biotinylated CBP501 derivative (bio-CBP501) were kindly provided by CanBas Co. Ltd (Shizuoka, Japan). Anti-14-3-3β, γ, ε, τ and ζ antibodies were obtained from Immunobiological Laboratories Co., Ltd (Gunma, Japan). T7-tag monoclonal antibody was purchased from Merck KGaA (Darmstadt, Germany). Anti-mouse IgG antibody HRP conjugated were purchased from Vector Laboratories, Inc. (Burlingame, CA). Anti-mouse and anti-rabbit IgG AP conjugated was purchased from Cell signaling technology, Inc. (Danvers, MA).

2.2. Screening of a library of T7 phage-displayed peptide

Screening of a library of T7 phage-displayed peptides was performed according to the previous reports[36–38] using bio-CBP501 and a Reacti-Bind™ NeutrAvidin™ Coated Plate, High Binding Capacity (PIERCE, Rockford, IL).

2.3. Peptide synthesis and purification

CBP501-binding peptide A2 (NSDCIISRKIEQKE), which was identified by a T7 phage display screen, was synthesized by the Fmoc method using a peptide synthesizer PS-3 (Aloka, Tokyo, Japan) and purified using a reverse phase preparative HPLC, as reported previously.[36,39]

2.4. Similarity search

We searched for candidate CBP501-binding proteins using Position-Specific Iterated Basic Local Alignment Search Tool (PSI-BLAST, NCBI) (http://www.ncbi.nlm.nih.gov/blast/Blast.cgi).

2.5. Production of recombinant 14-3-3ε, αCD and ΔCD protein

Recombinant 14-3-3ε, αCD and ΔCD proteins were engineered using pET28a(+) vector and host *Escherichia coli* BL21(DE3) pLysS. Each transformant was grown in 150 ml of Luria-Bertani (LB) medium containing 1% (w/v) glucose, 50 μg/ml of kanamycin and 34 μg/ml of chloramphenicol. Cells were grown and treated with 1 mM isopropyl thio-β-glactopyranoside (IPTG). Cells were harvested after 3 h by centrifugation at 3000*g* for 10 min. After removing the supernatant, the cell paste was frozen using liquid nitrogen and then stored at −80 °C until use. Cells were sonicated in binding buffer (20 mM phosphate, pH 7.4, 500 mM NaCl, 10 mM imidazole

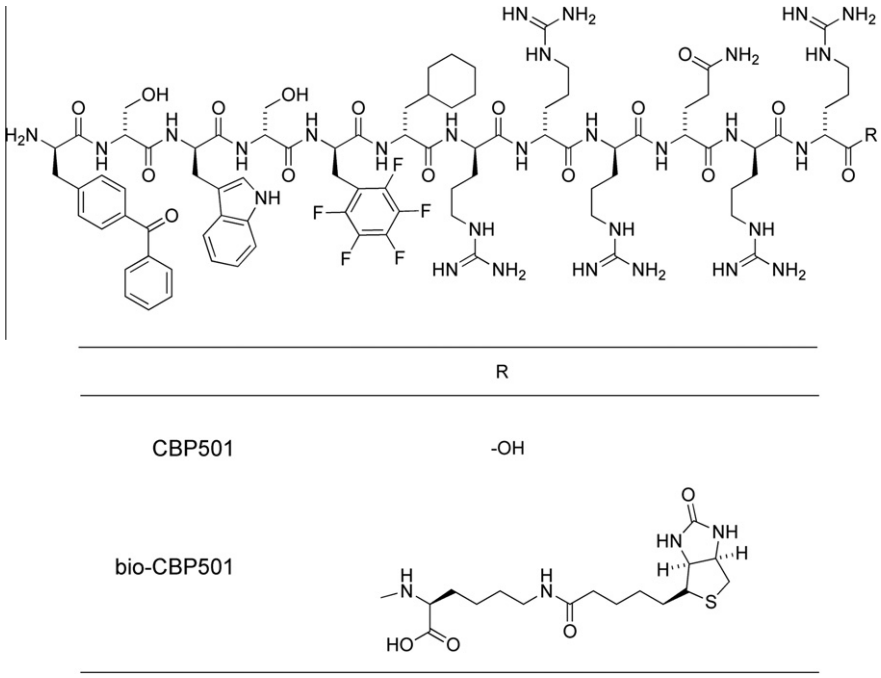

Figure 1. Structure of CBP501 and the biotinylated CBP501 derivative.

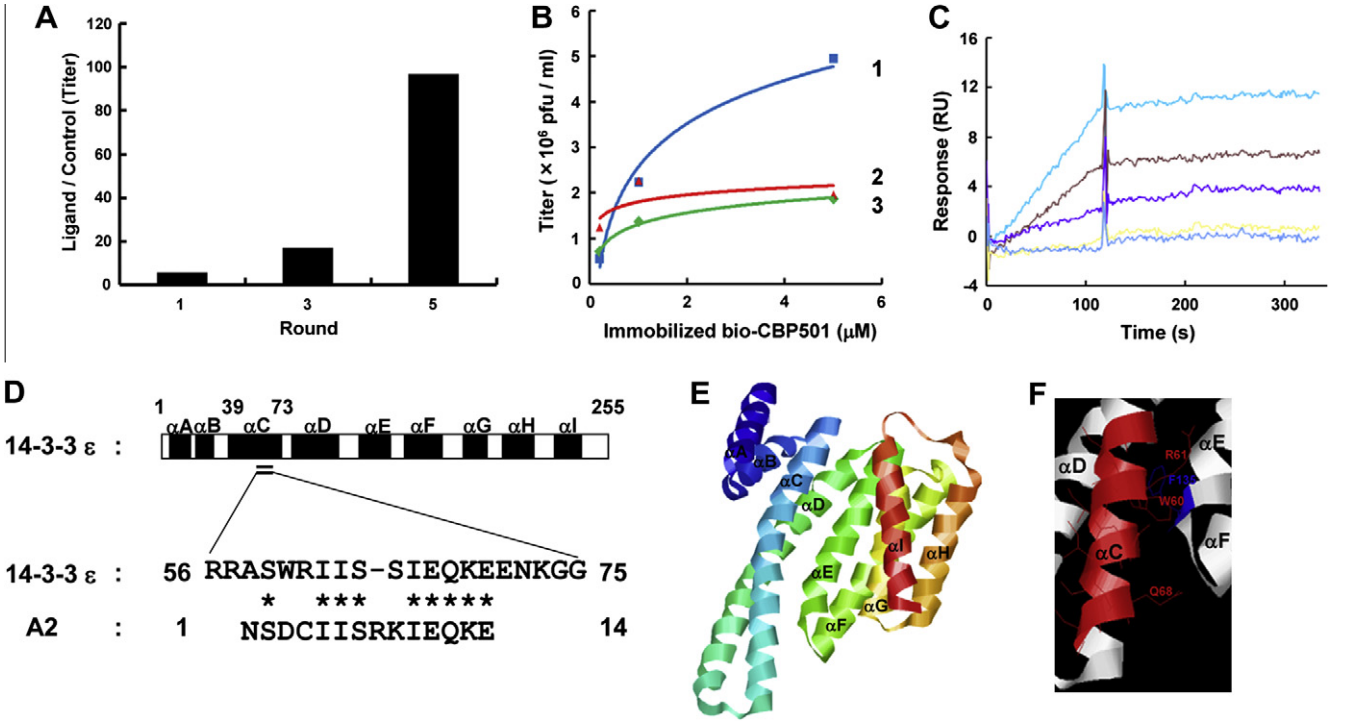

Figure 2. Screening of a library of T7 phage-displayed peptides for candidates that specifically recognizeCBP501. (A) Enrichment of the population of T7 phages by biopanning for CBP501. The bio-CBP501 immobilized well was allowed to react with the T7 phage library overnight at 4 °C. In every round, unbound phage was removed by washing five times with 100 mM Tris–HCl. Bound phage was eluted using 100 mM Tris–HCl containing 3 M NaCl. A non-bio-CBP501 immobilized well was used as a control. The data is shown as the ratio of titer from the eluted fraction (pfu) of ligand well/control well. (B) Comparison of affinity for CBP501 of selected phage (A2) versus control phage (E4, B4). Each line shows 1: A2, 2: B4 and 3: E4. (C) Binding analysis between the selected peptide sequence and CBP501 by SPR. CBP501 was immobilized on CM5 sensor chip and A2 peptide (6.25–100 μM) was injected. (D) Alignment between A2 amino acid sequence and 14-3-3ε. The amino acid sequence of A2 showed similarity to a part of the alphaC-helix region (A58-E70) of human 14-3-3ε. Three dimensional structure of human 14-3-3ε [PDB ID: 2br9]. (F) Magnification of the A2-like portion in alphaC helix.

(Im), 1 mM phenylmethylsulfonyl fluoride (PMSF), 1 μg/ml leupeptin) and centrifuged at 20,400*g* for 30 min. The supernatant was filtered using a PVDF membrane (Millex, pore size 0.22 μm; Millipore, Billerica, MA) and then loaded onto a 5 mL His-Trap HP column (GE Healthcare, Piscataway, NJ) pre-equilibrated with binding buffer. The column was washed in turn with 50 ml of wash buffer 1 (20 mM phosphate, pH 7.4, 500 mM NaCl, 40 mM Im) and wash buffer 2 (20 mM phosphate, pH 7.4, 500 mM NaCl, 80 mM Im). Bound proteins were then eluted using an FPLC system (ÄKTA prime plus, GE Healthcare, Uppsala, Sweden) on a linear gradient from 80 mM Im (0 min) to 500 mM Im (100 min) with a flow rate of 0.5 ml/min.

2.6. Measurement of circular dichroism (CD) spectra

Conformation of recombinant 14-3-3ε following purification was assigned by CD analysis. The CD spectra, at wavelengths between 200 and 250 nm, were obtained using a JASCO J800 spectropolarimeter (Jasco Corporation, Tokyo, Japan). Recombinant 14-3-3ε was diluted with a buffer (20 mM phosphate, pH 7.4, 500 mM NaCl) to a concentration of about 15 μM prior to CD analysis. An optical path length of 0.1 cm was employed for all measurements. The settings for the spectropolarimeter were as follows: step resolution 0.1 nm, scan speed 50 nm/min, response time 2 s, bandwidth 1 nm, and sensitivity 20 m deg. Spectrum was an accumulation of four individual scans.

2.7. SPR analysis between CBP501 and a 14-mer peptide or 14-3-3ε

Binding analysis between CBP501 and synthetic peptide/14-3-3ε was performed with a SPR biosensor (Biacore®3000, GE Healthcare, Piscataway, NJ).[40,41] Immobilization of CBP501 on a CM5 sensor chip surface was performed as previously described.[36,39] This reaction immobilized about 2000–4400 resonance units (RU) of CBP501.

Table 1
Kinetic parameters obtained from SPR analysis

No.	Ligand (fixed on CM5)	Analyte (injection)	k_a (M^{-1} s^{-1})	k_d (s^{-1})	K_D (k_d/k_a) (M)	R_{max} (RU)
1	CBP501	A2	1.1×10^1	9.6×10^{-6}	1.8×10^{-7}	77
2	CBP501	E4 (Cont.)	1.3	3.3×10^{-3}	2.6×10^{-3}	3490
3	CBP501	14-3-3ε	1.4×10^3	6.8×10^{-5}	4.8×10^{-8}	367
4	14-3-3ε	CBP501	1.6×10^4	5.8×10^{-2}	4.3×10^{-6}	755
5	14-3-3ε	CBP004	1.9×10^4	1.2×10^{-1}	6.3×10^{-6}	1610
6	14-3-3ε	TAT-S216A	7.0×10^3	1.8×10^{-1}	2.6×10^{-5}	450
7	14-3-3ε	UCN-01	1.0×10^3	1.3×10^{-1}	1.3×10^{-4}	239
8	14-3-3ε	SB218078	–	–	–	–
9	14-3-3ε	DBH	–	–	–	–

BIAevaluation 4.1 software (Biacore AB) was used to determine the parameters.
Analytical conditions: 50 mM phosphate buffer pH 7.4, 150 mM NaCl, 8% DMSO (Nos. 1–3), PBS, 5% DMSO (Nos. 4–9), 25 °C. k_a: association rate constant, k_d: dissociation rate constant, K_D: dissociation constant, R_{max}: maximum binding amounts calculated by global fitting.

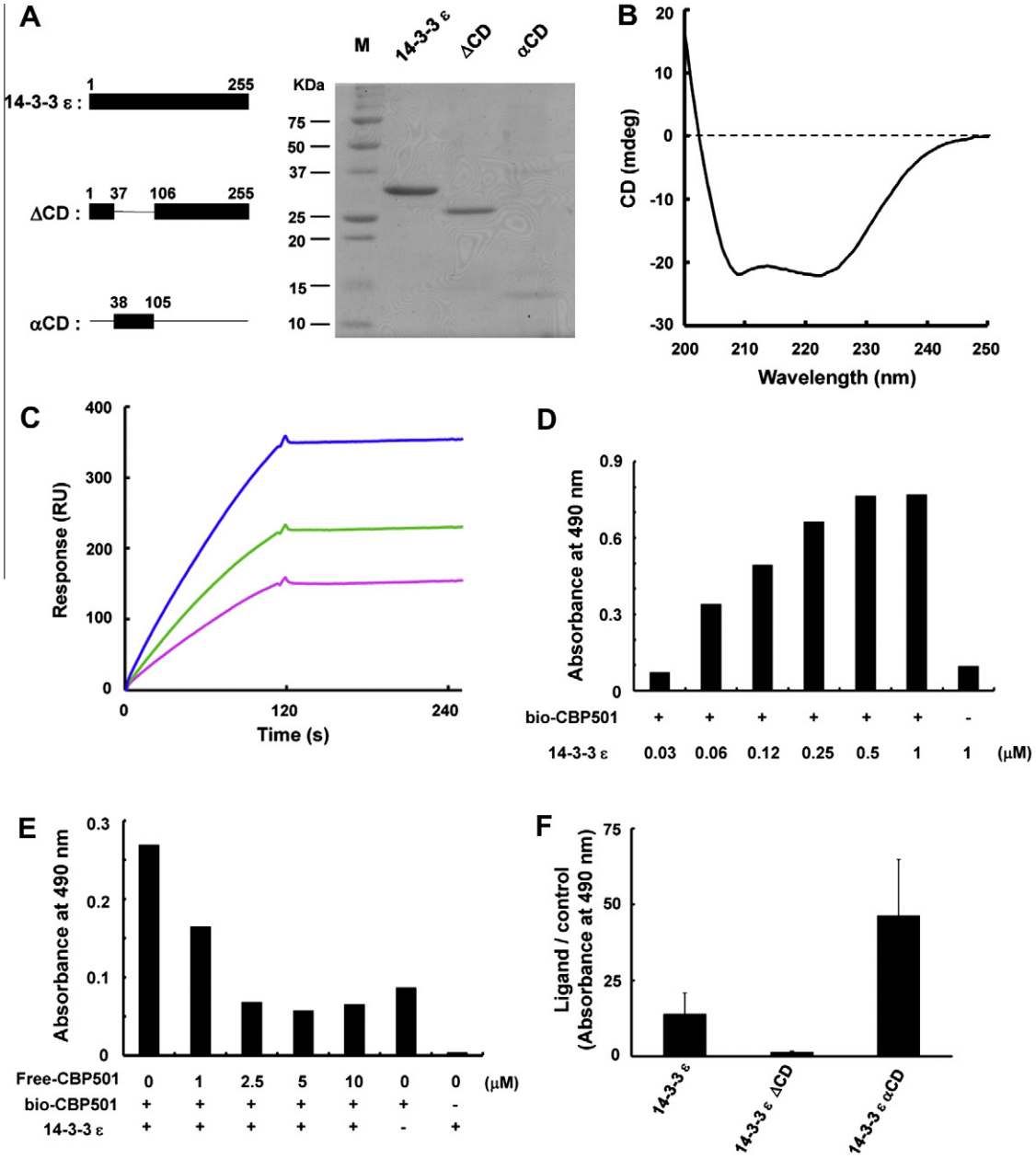

Figure 3. Expression and purification of recombinant His-tagged proteins and binding analysis between recombinant proteins and CBP501. (A) Simplified diagram of recombinant 14-3-3ε, αCD and ΔCD protein. Recombinant His-tagged proteins were expressed and purified. The apparent molecular weight of each protein as determined by SDS–PAGE was in good agreement with the predicted molecular weight based on the amino acid sequence. (B) CD spectrum of recombinant 14-3-3ε. (C) Binding analysis between recombinant 14-3-3ε and CBP501 by SPR. CBP501 was immobilized on CM5 sensor chip and recombinant 14-3-3ε (3.13–12.5 μM) was injected. (D) ELISA. Bio-CBP501 was immobilized for 1 h on a Reacti-Bind™ NeutraAvidin™ Coated Plate, High Binding Capacity (PIERCE). 14-3-3ε was added on the well in the presence (+) or the absence (−) of 1 μM bio-CBP501. (E) Competition assay. 14-3-3ε 0.125 μM) and each concentration of free-CBP501 were mixed and incubated for 1 h beforehand. The mixture was then addedto1 μM bio-CBP501-immobilized (+) or non-immobilized (−) well. (F) Scanning for CBP501-binding region in 14-3-3ε. 1 μM of protein was used for each experiment. The data is shown as the ratio of OD at 490 nm of 1 μM bio-CBP501-immobilized well versus non-immobilized well.

Binding analysis was performed by injecting synthetic A2 peptide (6.25–100 μM) in a running buffer (50 mM sodium phosphate, 150 mM NaCl, pH 7.0) with 8% DMSO or recombinant 14-3-3ε (3.125, 6.25, 12.5 μM) in HBS-EP running buffer (GE Healthcare), using a flow rate of 20 μl/min at 25 °C. Association time was setup at 120 s and dissociation time at 500 s. BIAevaluation 4.1 software (Biacore AB) was used to determine the kinetic parameters.

2.8. Comparison of affinity between Chk kinase inhibitors and 14-3-3ε

Recombinant 14-3-3ε (14,000 RU) was immobilized on a CM5 sensor chip by an amine coupling reaction. Binding analysis was performed by injecting Chk kinase inhibitor at various concentrations (0–20 μM) in PBS with 5% DMSO using a flow rate of 20 μl/min at 25 °C. Association time was setup at 120 s and dissociation time at 120 s. BIAevaluation 4.1 software (Biacore AB) was used to determine the kinetic parameters.

2.9. Elisa

The bio-CBP501 (1 mM, 100 μl) was immobilized on a Reacti-Bind™ NeutraAvidin™ Coated Plate, High Binding Capacity (PIERCE) by rotating gently for 1 h. The wells were blocked with 200 μl of PBS containing 1% (w/v) skimmed milk for 1.5 h and then washed twice with PBS. A 100 μl aliquot of recombinant 14-3-3ε,

αCD or ΔCD protein solution was individually associated with immobilized bio-CBP501 for 3 h. Nonspecifically bound proteins were removed by three washes with PBS and the remaining protein was detected using T7-tag monoclonal antibody as a primary antibody and anti-mouse IgG HRP conjugate as a secondary antibody. After the coloring reaction using *o*-phenylenediamine, absorbance at 490 nm was measured using an absorption spectrometer (NJ-2300, Inter Med, Tokyo, Japan) to detect the 14-3-3ε binding to the immobilized CBP501.

2.10. RT-PCR

Total-RNA was extracted from Jurkat cells using Sepasol-RNA I Super (Nacalai Tesque, Kyoto, Japan) according to the manufacturer's instructions. The DNA of each 14-3-3 isoform was amplified using primers as reported previously.[42] RT-PCR was carried out under the following conditions using SuperScript™ One-Step RT-PCR with Platinum Taq (Invitrogen): 50 °C for 30 min, 94 °C for 2 min, followed by 30 cycles of 94 °C for 40 s, 55 °C for 50 s and 72 °C for 60 s and finally one step at 72 °C for 7 min. A 10 μl aliquot of the amplified product was analyzed by agarose gel electrophoresis (1% gel).

2.11. Avidin-agarose bead pull-down assay

Whole cell lysate from Jurkat cells was generated using M-PER® Mammalian Protein Extraction Reagent (PIERCE) according to the manufacturer's instructions. The soluble fraction was incubated with 50 μl of avidin-agarose bead at 4 °C for 1 h on a rotary device to remove the nonspecifically bound proteins. Following centrifugation at 20,400*g* for 5 min, 100 μl of supernatant was incubated with or without bio-CBP501 (50 μM, 200 μl) at 4 °C for 3 h on a rotary device, and then with avidin-agarose beads (Sigma–Aldrich, St. Louis, MO) for 1 h to form the biotin–avidin complex. The complexes were pulled down by centrifugation at 2300*g* for 5 min and washed three times with 500 μl of PBS. Pellets were resuspended in 100 μl of SDS sample buffer (50 mM Tris–HCl, pH 6.8, 2% (w/v) SDS, 5% (v/v) β-mercaptoethanol, 10% (v/v) glycerol, 0.02% (w/v) bromophenol blue) and boiled at 95 °C for 15 min to dissociate the binding protein. After the removal of beads by centrifugation at 20,400*g* for 5 min, a 20 μl aliquot of the supernatant was applied to SDS–PAGE using a 12.5% separation gel. The 14-3-3 protein was detected by immunoblotting using monoclonal antibody for each isoform.

3. Results and discussion

3.1. Screening of a library of T7 phage-displayed peptides for candidates that specifically bind to CBP501

A T7 phage library was applied onto streptavidin-coated wells bearing an immobilized bio-CBP501 (Fig. 1). We determined the effective biopanning conditions by repeated rounds of selection using wash buffer with 100 mM Tris–HCl (pH 7.5) and elution buffer with 100 mM Tris–HCl (pH 7.5) with 3 M NaCl. As shown in Figure 2A, the recovery rate of round 5 (i.e. the eluted fraction of the 5th biopanning) was almost 90-fold higher than that from the control well. A random selection of phage clones from the fifth round of selection was arbitrarily picked from the eluate and the phage DNA sequence encoding the displayed peptide sequenced. Of the several peptide sequences detected, a 14-mer peptide NSDCIISRKIEQKE (hereafter referred to as 'A2') showed significant affinity in proportion to the concentration of CBP501 immobilized on a neutroavidin-coated 96-well microplate. The A2-displayed T7 phage showed a ~5-fold increase in titer over that of the control clones 'B4 (NS)' and 'E4 (NSPAGISRELVDKLAAALE)' at 5 μM of bio-CBP501 (Fig. 2B). This data indicated that 'A2' phage was effectively enriched in the biopanning procedure, presumably due to selective binding to CBP501.

Binding between CBP501 and synthetic A2 peptide was tested using a SPR biosensor (Biacore®3000). Figure 2C shows the

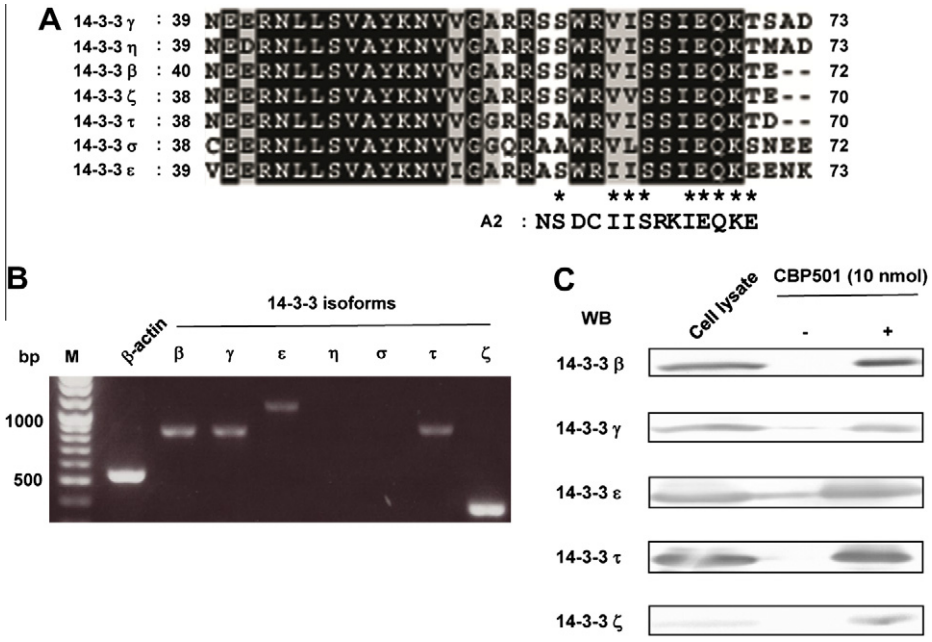

Figure 4. Interaction between CBP501 and other 14-3-3 isoforms. (A) Part of the amino acid sequence of the conserved alphaC helix in 14-3-3 displaying similarity to A2 peptide. (B) Detection of 14-3-3 mRNA in Jurkat cells. Cells were harvested by centrifugation and total-RNA was then extracted. RT-PCR was performed using the total RNA as template. The amplified product was then analyzed by agarose gel electrophoresis. (C) Detection of the interaction between CBP501 and 14-3-3. Jurkat cell lysates were incubated with bio-CBP501 and then complexed with avidin-agarose beads and centrifuged. The pellet was boiled with SDS sample buffer and then subjected to SDS–PAGE and immunoblotting. The antibody for each 14-3-3 isoform was used for detection.

sensorgram obtained between immobilized CBP501 on the CM5 sensor chip and various concentrations of A2 peptide injected over the sensor chip. Global fitting of this sensorgram was performed using BIAevaluation 4.1 software. The dissociation constant (K_D) between CBP501 and A2 peptide was1.8×10^{-7} M, compared with 2.6×10^{-3} M between CBP501 and control E4 peptide (Table 1). Therefore, A2 peptide specifically binds to CBP501 with a strong affinity, which supports the result of the T7 phage display screen.

Using BLAST and the sequence of A2 peptide as a query, we selected candidate proteins relevant to the G2 checkpoint that possesses a similar segment of sequence to that of peptide A2. Among the large number of potential positive hits, 14-3-3ε protein was listed as a candidate. As shown in Figure 2D–F, amino acid sequence within apart of the alphaC helix of 14-3-3ε is similar to that of A2 peptide, suggesting that CBP501 may bind to this region. Furthermore, secondary structure prediction program (IBCP, France)[43] predicted that A2 peptide possesses a potential αhelix structure, which supports this hypothesis (data not shown).

3.2. CBP501 binds to 14-3-3ε via the alphaC helix that displays sequence similarity to the A2 peptide

Next, we aimed to test the proposed interaction between CBP501 and 14-3-3ε protein. His-tagged full length 14-3-3ε and truncated versions of the protein (ΔCD and αCD) were engineered and purified by Ni^+ affinity column chromatography (Fig. 3A). The measurement of CD spectra of full length 14-3-3ε showed the negative peak at wavelength 207 nm (Fig. 3B), indicating the presence of alpha helices and the correct folding into the proposed structure (Fig. 2E). The binding experiments using SPR analysis (Fig. 3C) and ELISA (Fig. 3D) clearly demonstrated that CBP501 binds to 14-3-3ε in a dose-dependent manner. The K_D value obtained from SPR analysis was 4.8×10^{-8} M (Table 1), suggesting a strong interaction between CBP501 and 14-3-3ε. Interaction between immobilized CBP501 and 14-3-3ε was prevented by pre-incubating 14-3-3ε with free-CBP501 for 1 h beforehand (Fig. 3E). Furthermore, the binding of CBP501 to 14-3-3ε was

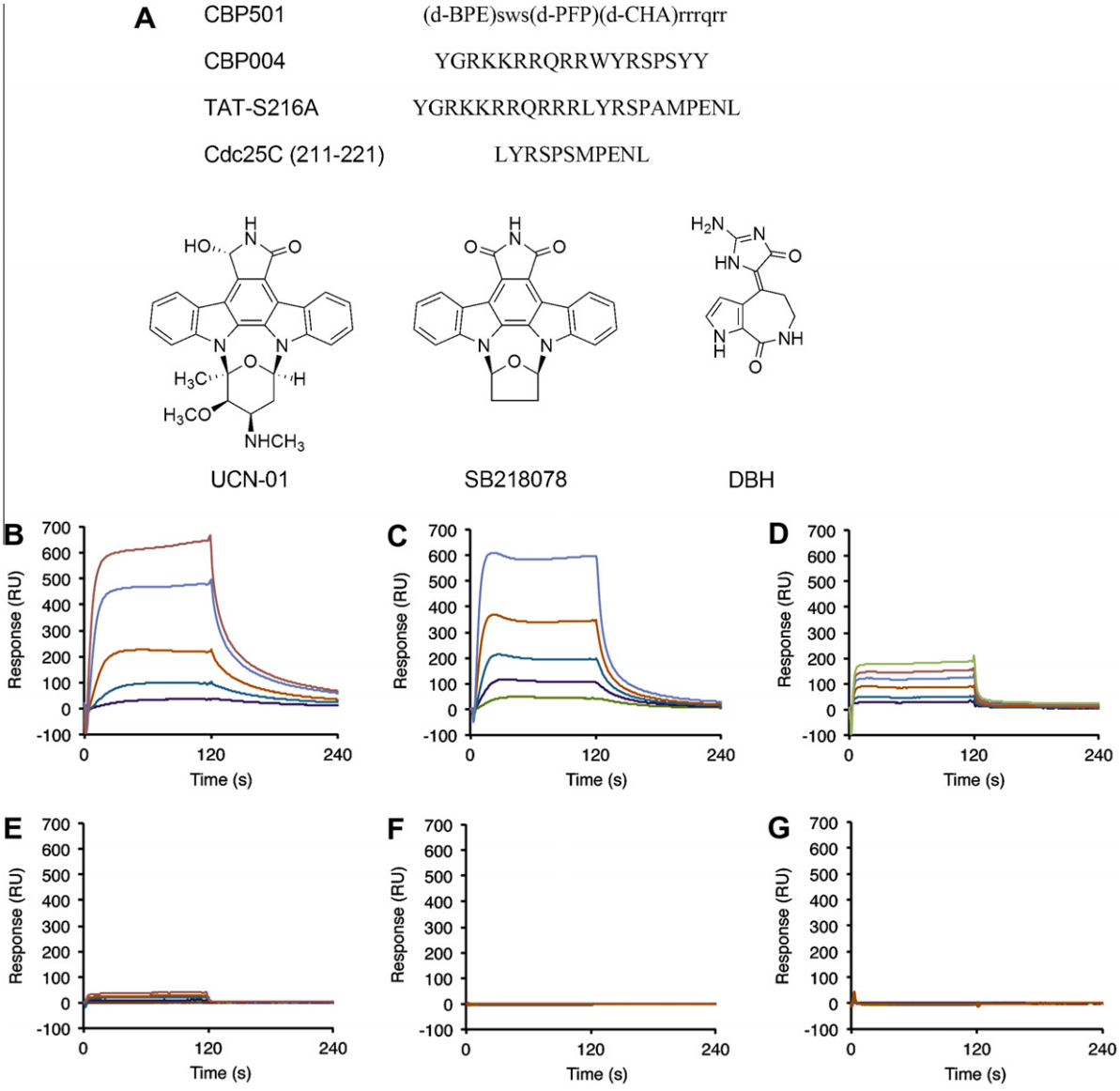

Figure 5. SPR analysis between Chk kinase inhibitors and immobilized 14-3-3ε. (A) Sequence and structure of Chk kinase inhibitor. Amino acids in capital letter symbols indicate L-type amino acid, whereas those given as small letters indicate D-type amino acids. D-BPE, D-*p*-benzoylphenylalanyl; D-PFP, D-pentafluorophenylalanyl; D-CHA, D-cyclohexylalanyl. (B) SPR sensorgram between CBP501 (0.5, 1, 2, 4 and 6 μM) and immobilized 14-3-3ε. (C) CBP004 (0.25, 0.5, 1, 2 and 4 μM). (D) TAT-S216A (1, 2, 4, 6, 8 and 10 μM). (E) UCN-01 (1, 2, 4, 6, 8 and 10 μM). (F) SB218078 (1, 2.5, 5, 7.5 and 10 μM). (G) DBH (1, 2.5, 5, 7.5 and 10 μM).

decreased by the loss of the region from T38 to D105 (ΔCD), whereas CBP501 showed the strongest binding against T38-D105 polypeptide (αCD) (Fig. 3F). From these data, it is likely that CBP501 binds to 14-3-3ε protein via the amino acids corresponding to T38-D105. Part of the alphaC helix within 14-3-3ε is known to be significant as a scaffold of homo- and heterodimerization of this protein, which leads to subsequent interactions with other target proteins. Furthermore, the polypeptide portion containing F135, which is important for 14-3-3ε binding to other proteins,[19] is sterically close to this alphaC helix, comprising a cavity that other proteins can directly associate with during homo- or heterodimerization (Fig. 2F). Thus, binding of CBP501 to this site in 14-3-3ε seems to be biologically significant in terms of the G2 checkpoint.

3.3. Evidence that CBP501 binds to cellular 14-3-3 proteins

In order to demonstrate the binding of CBP501 to 14-3-3ε, we attempted to extract 14-3-3ε from the soluble fraction of Jurkat cells using bio-CBP501 and avidin-agarose bead. The region of alphaC helix similarity to A2 peptide is also conserved in β, γ, η, ζ, σ and τ of human 14-3-3 isoforms (Fig. 4A). Thus, we further verified whether the other isoforms bind with CBP501. As shown in Figure 4B, 14-3-3β, γ, τ and ζ gene expression was detected by RT-PCR in addition to the ε isoform in Jurkat cells. Pull-down assays of cell lysates and subsequent immunoblotting confirmed that CBP501 directly interacts with 14-3-3ε and other isoforms present in Jurkat cells (Fig. 4C).

Interestingly, 14-3-3σ, an important mediator in the p53-mediated G2 checkpoint pathway, was not expressed in Jurkat cells in addition to the η isoform (Fig. 4B). The σ isoform seems to be irrelevant with regard to G2 abrogation of CBP501 in Jurkat cells, despite the presence of a CBP501-binding site (Fig. 4A). Rather, subtypes involved in Cdc25-mediated pathway may be related to the activity of CBP501. Indeed, it was reported that 14-3-3ε and γ are important for forming a complex with Cdc25C.[19,21–24] Likewise, with the exception of σ, 14-3-3 isoforms are also essential for associating with Chk1 or Wee1 and regulating G2 checkpoint pathway, although details should be further clarified.[25–30] It is also of interest that each isoform plays an intrinsic role in the G2 checkpoint, despite the highly conserved primary and tertiary structures among 14-3-3 isoforms. Moreover, CBP501 alone does not show any effect up to a concentration of 12.5 μM.[32] Thus, in order to elucidate the relationship between G2 arrest by CBP501 and binding of CBP501 to 14-3-3, functional differences of 14-3-3 isoforms on the G2 checkpoint as well as the 14-3-3-mediated crosstalk in the presence of DNA-damaging agents need to be clarified in detail.

3.4. Comparison of the affinity between 14-3-3ε and Chk kinase inhibitors by SPR analysis

To investigate the binding specificity and affinity strength between CBP501 and 14-3-3ε, we tested the interaction between 14-3-3ε and well-known Chk kinase inhibitors (Fig. 5A) using an SPR biosensor. Our analysis revealed that CBP501 bound to 14-3-3ε (Fig. 5B), regardless of which species was immobilized (see Fig. 2C). However, the shape of the sensorgram and kinetic parameters in these experiments was different depending on whether 14-3-3ε was the ligand or analyte. This observation could be rationalized in terms of a required alteration in flexibility of each molecule during the association and dissociation process. CBP004 contains a similar sequence to residues 211–221 of Cdc25C that comprises the 14-3-3-binding site by S216 phosphorylation (Fig. 5A).[32] As expected, CBP004 associated with 14-3-3ε and showed a more rapid dissociation profile (k_d: 1.2×10^{-1} s^{-1}) than that of CBP501 (k_d: 5.8×10^{-2} s^{-1}) (Fig. 5B and C, Table 1). TAT-S216A, which is the original template of CBP501 and contains a sequence corresponding to residues 211–221 of Cdc25C (Fig. 5A), also interacted with 14-3-3ε, although the affinity was considerably weaker than that of CBP501.Indeed, the sensorgram showed a square-shaped response, suggesting weak interaction (Fig. 5D, Table 1). UCN-01 also responded little against the immobilized 14-3-3ε (Fig. 5E, Table 1). By contrast, SB218078 and DBH did not respond at all within the concentration range tested (Fig. 5F and G). Thus, the affinity against 14-3-3ε was the strongest for CBP501 among the Chk kinase inhibitors tested. It must be emphasized that the sequence of CBP501, which comprises D-amino acids as well as unnatural amino acids, is quite different to residues 211–221 of Cdc25C (Fig. 5A).

4. Conclusion

In this study, we have identified a CBP501-binding peptide NSDCIISRKIEQKE by the use of T7 phage display technology. A similarity search and subsequent binding analysis using SPR biosensor and ELISA revealed the alphaC helix in 14-3-3ε as a CBP501-binding site. In addition, we demonstrated that CBP501 also bound to other 14-3-3 isoforms from Jurkat cells and the affinity was the strongest among the Chk kinase inhibitors tested. Our results provide a platform for further studies to investigate the molecular mechanism of action of CBP501. Furthermore, our experimental strategy involving screening a library of T7 phage-displayed peptides combined with a subsequent similarity search is a promising methodology for determining drug-binding sites on proteins as well as identifying candidate biological targets.

Acknowledgment

This work was supported in part by a research grant from CanBas Co. Ltd.

References and notes

1. Houtgraaf, J. H.; Versmissen, J.; van der Giessen, W. J. *Cardiovasc. Revasc. Med.* **2006**, *7*, 165.
2. Hartwell, L. H.; Weinert, T. A. *Science* **1989**, *246*, 629.
3. Kastan, M. B.; Bartek, J. *Nature* **2004**, *432*, 316.
4. Elledge, S. J. *Science* **1996**, *274*, 1664.
5. Paulovich, A. G.; Toczyski, D. P.; Hartwell, L. H. *Cell* **1997**, *88*, 315.
6. Harrington, E. A.; Bruce, J. L.; Harlow, E.; Dyson, N. *Proc. Natl. Acad. Sci. U.S.A.* **1998**, *95*, 11945.
7. Levine, A. J. *Cell* **1997**, *88*, 323.
8. Sherr, C. J. *Science* **1996**, *274*, 1672.
9. Khanna, K. K.; Beamish, H.; Yan, J.; Hobson, K.; Williams, R.; Dunn, I.; Lavin, M. F. *Oncogene* **1995**, *11*, 609.
10. Smith, M. L.; Zhan, Q.; Bae, I.; Fornace, A. J., Jr. *Exp. Cell Res.* **1994**, *215*, 386.
11. Abraham, R. T. *Gene Dev.* **2001**, *15*, 2177.
12. Graves, P. R.; Lovly, C. M.; Uy, G. L.; Piwnica-Worms, H. *Oncogene* **2001**, *20*, 1839.
13. Lopez-Girona, A.; Furnari, B.; Mondesert, O.; Russell, P. *Nature* **1999**, *397*, 172.
14. Levesque, A. A.; Fanous, A. A.; Poh, A.; Eastman, A. *Mol. Cancer Ther.* **2008**, *7*, 252.
15. Wilker, E. W.; Grant, R. A.; Artim, S. C.; Yaffe, M. B. *J. Biol. Chem.* **2005**, *280*, 18891.
16. Chan, T. A.; Hermeking, H.; Lengauer, C.; Kinzler, K. W.; Vogelstein, B. *Nature* **1999**, *401*, 616.
17. Hermeking, H.; Benzinger, A. *Semin. Cancer Biol.* **2006**, *16*, 183.
18. Yang, X.; Lee, W. H.; Sobott, F.; Papagrigoriou, E.; Robinson, C. V.; Grossmann, J. G.; Sundstrom, M.; Doyle, D. A.; Elkins, J. M. *Proc. Natl. Acad. Sci. U.S.A.* **2006**, *103*, 17237.
19. Telles, E.; Hosing, A. S.; Kundu, S. T.; Venkatraman, P.; Dalal, S. N. *Exp. Cell Res.* **2009**, *315*, 1448.
20. Dougherty, M. K.; Morrison, D. K. *J. Cell Sci.* **2004**, *117*, 1875.
21. Hosing, A. S.; Kundu, S. T.; Dalal, S. N. *Cell Cycle* **2008**, *7*, 3171.
22. Konishi, H.; Nakagawa, T.; Harano, T.; Mizuno, K.; Saito, H.; Masuda, A.; Matsuda, H.; Osada, H.; Takahashi, T. *Cancer Res.* **2002**, *62*, 271.
23. Sanchez, Y.; Wong, C.; Thoma, R. S.; Richman, R.; Wu, Z.; Piwnica-Worms, H.; Elledge, S. J. *Science* **1997**, *277*, 1497.
24. Peng, C. Y.; Graves, P. R.; Thoma, R. S.; Wu, Z.; Shaw, A. S.; Piwnica-Worms, H. *Science* **1997**, *277*, 1501.

25. Rothblum-Oviatt, C. J.; Ryan, C. E.; Piwnica-Worms, H. *Cell Growth Differ.* **2001**, *12*, 581.
26. Lee, J.; Kumagai, A.; Dunphy, W. G. *Mol. Biol. Cell* **2001**, *12*, 551.
27. Wang, Y.; Jacobs, C.; Hook, K. E.; Duan, H.; Booher, R. N.; Sun, Y. *Cell Growth Differ.* **2000**, *11*, 211.
28. Honda, R.; Ohba, Y.; Yasuda, H. *Biochem. Biophys. Res. Commun.* **1997**, *230*, 262.
29. Dunaway, S.; Liu, H. Y.; Walworth, N. C. *J. Cell Sci.* **2005**, *118*, 39.
30. Chen, L.; Liu, T. H.; Walworth, N. C. *Gene Dev.* **1999**, *13*, 675.
31. Kawabe, T. *Mol. Cancer Ther.* **2004**, *3*, 513.
32. Sha, S. K.; Sato, T.; Kobayashi, H.; Ishigaki, M.; Yamamoto, S.; Sato, H.; Takada, A.; Nakajyo, S.; Mochizuki, Y.; Friedman, J. M.; Cheng, F. C.; Okura, T.; Kimura, R.; Kufe, D. W.; Vonhoff, D. D.; Kawabe, T. *Mol. Cancer Ther.* **2007**, *6*, 147.
33. Suganuma, M.; Kawabe, T.; Hori, H.; Funabiki, T.; Okamoto, T. *Cancer Res.* **1999**, *59*, 5887.
34. Shapiro, G. I.; Tibes, R.; Gordon, M. S.; Wong, B. Y.; Eder, J. P.; Borad, M. J.; Mendelson, D. S.; Vogelzang, N. J.; Bastos, B. R.; Weiss, G. J.; Fernandez, C.; Sutherland, W.; Sato, H.; Pierceall, W. E.; Weaver, D.; Slough, S.; Wasserman, E.; Kufe, D. W.; Von Hoff, D.; Kawabe, T.; Sharma, S. *Clin. Cancer Res.* **2011**, *17*, 3431.
35. Takakusagi, Y.; Takakusagi, K.; Sugawara, F.; Sakaguchi, K. *Expert Opin. Drug Discov.* **2010**, *5*, 361.
36. Takami, M.; Takakusagi, Y.; Kuramochi, K.; Tsukuda, S.; Aoki, S.; Morohashi, K.; Ohta, K.; Kobayashi, S.; Sakaguchi, K.; Sugawara, F. *Molecules* **2011**, *16*, 4278.
37. Takakusagi, Y.; Takakusagi, K.; Kuramochi, K.; Kobayashi, S.; Sugawara, F.; Sakaguchi, K. *Bioorg. Med. Chem.* **2007**, *15*, 7590.
38. Takakusagi, Y.; Ohta, K.; Kuramochi, K.; Morohashi, K.; Kobayashi, S.; Sakaguchi, K.; Sugawara, F. *Bioorg. Med. Chem. Lett.* **2005**, *15*, 4846.
39. Takakusagi, Y.; Kuroiwa, Y.; Sugawara, F.; Sakaguchi, K. *Bioorg. Med. Chem.* **2008**, *16*, 7410.
40. Homola, J.; Koudela, I.; Yee, S. S. *Sens. Actuators, B Chem.* **1999**, *54*, 16.
41. Andersson, K.; Areskoug, D.; Hardenborg, E. *J. Mol. Recognit.* **1999**, *12*, 310.
42. Qi, W.; Liu, X.; Qiao, D.; Martinez, J. D. *Int. J. Cancer* **2005**, *113*, 359.
43. Deleage, G.; Blanchet, C.; Geourjon, C. *Biochimie* **1997**, *79*, 681.